Mach-Zehnder modulator modeling based on imec-ePixFab ISIPP25G SiPhotonics

Diego M. Dourado, Mônica L. Rocha and João Paulo P. Carmo
Electrical and Computer Engineering Department EESC, USP
São Carlos, Brazil
diego.dourado@usp.br

***Abstract*—This paper presents the design of a modulator using a silicon photonics technology known as ePixFab ISIPP25G. By modeling a Mach-Zehnder architecture, to achieve high modulation rates, and employing physical parameters and data for silicon waveguides taken from standard libraries, we demonstrate that, for a bit rate of 20 Gb/s, it is possible to dimension a modulator with a figure of merit equal to 0.95 V.cm to induce intensity modulation. In addition, to ensure the modulation format, an amplifier with a gain of 26 dB was inserted into the external circuit of the device. Finally, when configuring the arbitrary waveform generator (AWG) with pulse width equal to 25% of the period (square wave), it was possible to calculate the capacitive time constant (τ = 0.423 ps) and observe that the modulator achieves maximum modulation intensity by varying the voltage between 0 and 9.5 V on each arm of the structure. For this, the rise (10% to 90%) and fall (90% to 10%) times of the real modulation signal were calculated, where τ_r = 26.5 ps and τ_f = 10.8 ps were measured, respectively.**

***Index Terms*—silicon photonics, mach-zehnder modulator design, intensity and phase modulations**

I. Introduction

Due to the exponential increase in data consumption by fixed and mobile broadband subscribers, growing bandwidth demand by high-definition video services, silicon photonics devices emerges as a potential solution for future generations of optical fiber systems, from short-reach interconnect, metropolitan and access networks [1]. To understand the mechanisms of modulation in silicon, it is convenient to know that optical modulation is performed by devices that produce direct changes in optical intensity via absorption, or produce changes in the refractive index of the material used in the device. In this case, it is possible to use structures that allow conversion to a change of intensity, i.e. an interferometer (e.g. a Mach-Zehnder [2]) or a resonant device (e.g. a ring resonator [3]). In order to change the refractive index in the material, it is necessary to apply an electrical signal to the device. Moreover, the use of an electric field has become a fairly frequent means in the optical modulation process, so this will contribute to low or no current in the device and as a result, the modulator will have low energy expenditure and a fast response time [4].

The application of an electric field to a material can result in a change in the real refractive index (electro-refraction) and in a change in the imaginary refractive index (electro-absorption) [5]. In this way, it is possible to use different physical effects to modulate devices, for example: plasma dispersion effect [6], Pockels and Kerr effects [7], Franz-Keldysh effect (FKE) [8], Quantum Confined Stark effect (QCSE) [9] and thermo-optical effect [10].

Different optical modulators can be designed due to the wide variety of materials, optical devices and, mainly, some effects related to modulation mechanisms. By verifying the state of the art in modulators, a structure of great importance was chosen and discussed in this paper, which forms the bottleneck of the modulation means in the optical communication systems: the Mach-Zehnder Modulator (MZM) based on silicon photonics.

A. Objective and Organization

Among several scenarios of modulation in silicon photonics, the main objective of this paper was to explore and propose means of designing a modulator using technologies that are available in the market. Based on the Seimetz studies [11], intrinsic MZM parameters (e.g. length of the waveguide, figures of merit, among others) will be analyzed and proposed in order to achieve robust intensity modulation. In addition, the study suggests technical specifications and some electro-optical devices that can be used in the design of a symmetric Mach-Zehnder modulator.

The paper is organized in three parts, and section II deals with concepts of wave propagation in optical waveguides, specifically in silicon. In addition, knowing the technical parameters of the phase shifter block, the study covers steps that optimize the relation between the length of the waveguide and the voltage applied to the phase shifter. Then, after dimensioning the waveguides and adjusting the input voltages, a MZM has been configured to induce intensity modulation.

Section III discusses the simulation results and specifies the devices that can be used in practice in the modulation process.

The research received funding from CAPES.

978-1-5386-6702-6/18/$31.00 ©2018 IEEE

Finally, section IV presents a brief conclusion of the values obtained during the simulation.

II. Device Design Plan

A MZM can be designed from a Mach-Zehnder Interferometer (MZI), which is common in optical devices such as filters and switches. The architecture of a MZM employs waveguides in both input and output. In addition, adds in its basic structure a beam combiner and an optical beam splitter. Figure 1 shows the structure of a MZM, which receives a field (E_{in}) at the input of the waveguide and, in turn, will be splitted into two optical beams (E_A and E_B) that will follow the path in each arm of the device. In Fig. 1, it is also observed that in each arm of the structure are embedded phase shifters, highlighted in blue and red colors. Therefore, for the signal modulation to occur, it is necessary to apply a voltage to one or both phase shifters of the device. Thus, when the fields go through the arms of the structure and combine at the output of the modulator, a phase difference occurs between the two optical waves, producing intensity modulation or phase modulation in the output signal (E_{out}). In the specifications, the necessary driving voltage for achieving a phase shift equal to π radians, denoted as V_π, is typically given.

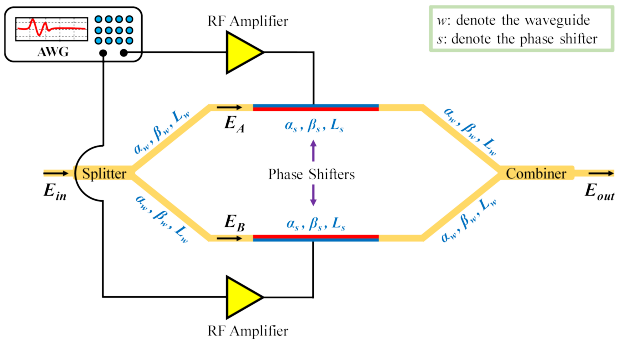

Fig. 1: Structure of the Mach-Zehnder modulator.

For a better understanding of the Mach-Zehnder's modulation mechanism, consider a wave (E_{in}) with TE polarization at the input of the waveguide, as shown in Fig. 1. Considering a symmetrical modulator and assuming that the signal is evenly splitted into each arm of the device, so that E_A and E_B carry the same intensity and travel along identical optical paths, it is feasible to represent the output signal (E_{out}) of the structure as a function of the input field (E_{in}), as shown in (4).

$$\beta_{w,s} = \frac{2\pi}{\lambda} n_{w,s} \tag{1}$$

$$E_{in} = E_0 \times e^{i2\pi ft} \tag{2}$$

$$E_{A,B} = \frac{E_{in}}{\sqrt{2}} \times e^{-i(2\beta_w L_w \pm \beta_s L_s) - \frac{\alpha_w}{2}(2L_w) - \frac{\alpha_s}{2} L_s} \tag{3}$$

$$E_{out} = \frac{1}{\sqrt{2}} \times (E_A + E_B) \tag{4}$$

in which β is the propagation constant of the light, α is the attenuation and L represents the length of material used in the device (see in Fig. 1). Note that the subscripts "w" and "s" of the parameters (α, β and L) present in (1) and (3), represent portions of the waveguide and phase shifter, respectively. In (1) it is observed that the constant β depends on the target wavelength (λ) and the refractive index (n) of the material medium.

In addition, with L being an independent parameter, only one optical structure is required to induce different modulation means by varying the length of the waveguide or by varying the voltage applied in the modulator. As one of the proposals of this paper, the following section discusses two modulation means that can be applied in the same symmetrical architecture showed in Fig. 1. Thus, by adjusting the voltage applied to the phase shifter and by dimensioning the waveguide length, the modulator can be configured in push-pull or push-push mode.

A. Modulator Dimensioning Method

An intensity or phase modulator can be manufactured as an integrated optical device by embedding two optical waveguides into an electro-optical substrate. In this way, when the material is subjected by an electric field, the Pockels effect causes a change in the real refractive index of the material, so that this change is proportional to the applied field. For this reason, the phenomenon is also known as a linear electro-optic effect. This event naturally depends on the polarization, that is, on the direction in which the electric field is applied in relation to the axes of the crystal structure [5].

Knowing that the Pockels effect does not occur in silicon, we simulate the behavior of its refractive index using the Lumerical commercial software and observe that its variation is very small ($\Delta n_s \sim 10^{-4}$) when a given voltage is applied in a medium doped silicon rib waveguide. Thus, for simplicity, the change of the refractive index was considered linear to the voltage applied in the phase shifters of the modulator. Therefore, the phase shift (ψ_s) in the modulator arms can be combined with Seimetz [11] equation and written as:

$$\psi_s = \beta_s L_s \approx \pm \frac{V_{RF}(t) + V_{DC}(t)}{V_\pi} \times \pi = \pm \frac{V_{in}(t)}{V_\pi} \times \pi \tag{5}$$

in which $V_{RF}(t)$ and $V_{DC}(t)$ are functions of the RF and DC voltages, respectively, applied to each arm of the device to produce a phase shift in the output signal. Note that in (5), by adjusting the input voltage V_{in} to be equal to V_π, the phase shift in one of the modulator arms will be π radians. Thus, given the structure of the phase shifter and knowing its value of V_π, the lengths of the waveguides that make up the MZM's arms can be estimated with certain precision.

Considering a MZM operating in push-pull mode, so that ψ_s in arm A is equal to $-\psi_s$ in arm B, when setting the V_{RF} amplitude to be equal to $V\pi$ and $V_{DC} = -V_\pi/2$, for example, it is possible to solve (6) for a phase shift $\psi_w = \beta_w L_w$ in the waveguide. In this way, a variety of L_w lengths can be

calculated according to the design of the modulator, as shown in (7).

$$-2\psi_w \pm \psi_s = \pm\frac{\pi}{2} \tag{6}$$

$$L_w = \frac{1}{\beta_w}\left(\frac{\pi}{2} + 2k\pi\right), \quad k \in Z_+ \tag{7}$$

With this theoretical method for the design of a symmetric MZM, a half-wave shift ($\pm\pi/2$ radians) is applied to each arm of the device. As a result, at some time a destructive interference will occur at E_{out} and an intensity modulation will be induced.

Otherwise, by making ψ_s in arm A equal to ψ_s in arm B, the modulator is operated in push-push mode. Thus, by adjusting the modulator's operating point (via V_{RF} and V_{DC}) and considering a phase shift equal to φ radians in each arm of the structure (see (8)), it is possible to estimate the length L_w of the waveguide that makes up the device by (9).

$$-2\psi_w - \psi_s = -\varphi \tag{8}$$

$$L_w = \frac{1}{\beta_w}\left(\frac{\varphi - \psi_s}{2} + 2k\pi\right), \quad k \in Z_+ \tag{9}$$

In this way, for each variation of the electric field in the phase shifter, if desired, the two arms of the modulator experience the same phase shift with relation to the input signal. Thus, the push-push modulation mode induces robust phase modulation in the output signal (E_{out}).

Once the modulator dimensioning method has been described, the following section will discuss the intrinsic characteristics of the MZM, including its complete design with an external circuit.

B. Application topology

Based on real parameters (e.g. figures of merit, attenuation, among others) of the optical components provided by IMEC [12], this part of the paper proposes the design of a push-pull modulator powered by an external circuit. Figure 2 shows the equivalent circuit of the phase shifter being powered by an external RF signal.

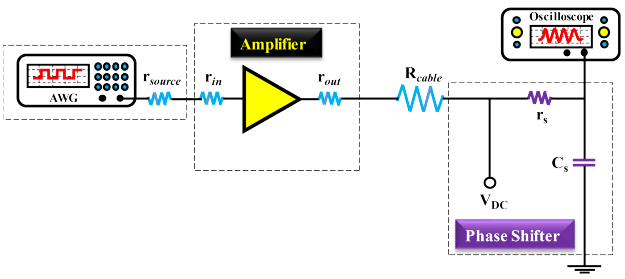

Fig. 2: RF and DC signals applied to the phase shifter, represented by its equivalent circuit.

All components in Fig. 2 were scaled in the Simulation and Model-Based Design software (SIMULINK). The arbitrary waveform generator (AWG) was configured to produce a square wave with a voltage equal to 1 V_{pp} and a bit rate equal to 20 Gb/s. The pulse width was set to 25% of the period and the resistance of the cables assumes the value of 50 Ω. Since the modulator requires at least V_{in} equal to 9.5 V to shift $\pi/2$ radians in each arm of the device, the DC bias voltage has been set to $-V_\pi/2$ and a power amplifier with a minimum gain of ∼24.59 dB was inserted into the system circuit.

The waveguide chosen was of the rib type, which can be embedded in a phase shifter based on a medium doping lateral PN junction. A laser with power equal to 1 mW operating at 1550 nm was inserted at the input of the modulator.

In this way, by scaling the electrical parameters of the external circuit with the optical parameters of the modulator, the device is ready to modulate the signal in amplitude or phase, depending on the application.

III. RESULTS

Combining techniques of optical modulation in silicon photonics proposed in section II-A with concepts applied in RF signals in section II-B, this section presents a general analysis of the results obtained during the simulations. For this reason, based on prior knowledge of the phase shifter block, section II-A discussed means for calculating the length of the waveguides when applying certain voltage on the modulator's arms.

Structured with commercially available components, Table I shows all the simulation parameters of the project and proposes two components (AWG and amplifier) for the practical implementation of the external RF circuit. In this way, using the dimensioning techniques proposed in section II-A, the optical components available in reference [12] (top of the Table I) can be combined with the external circuit model (bottom of the Table I) proposed in section II-B.

In Table I, it can be seen that the part of the system gain adjustment (≥24.59 dB) can be suppressed by the power amplifier inserted in the AWG output port. Moreover, for high bit rates, an AWG with a bandwidth equal to 25 GHz can be used during the modulation process.

As the waveguide length may vary according to the device's footprint, in this work L_w was dimensioned in 400 μm, which is a typical value used in designs of silicon photonic modulators. Moreover, high L_w values can increase the attenuation of the optical carrier and, as a result, compromise the output signal of the device and increase operating costs.

A. Output signal performance

When the RF signal is applied to the modulator's arms, a control signal, also applied to the phase shifter, is required, which establishes the operating point of the MZM. Such control signal is designated as DC bias voltage. In this way, it was possible to control the device and adjust its working mode during the signal modulation. Figure 3 shows the electric field and power transfer functions produced by the modulator operating in quadrature point.

TABLE I: Optical & Electrical components for the modulator design.

Optical characteristics of the modulator (extracted from [12])		
MZM	Device block	
Parameters	***Waveguide***	***Phase Shifter***
α	1.34 dB/cm	30 dB/cm
$V_\pi \times L$[a]	-	0.95 V.cm
L	Variable with k	0.5 mm
C/L	-	0.47 fF/μm
$R \times L$	-	0.9 Ω.mm
Main components of the proposed external circuit		
RF Signal	Device block	
	AWG	***Amplifier***
model	M8195A	HMC6981
Manufacturer	Keysight Technologies	Analog Devices
V_{pp}	1 V	-
Bandwidth	25 GHz	15-20 GHz
R	50 Ω	50 Ω Input/Output
Gain	-	26 dB
Output IP3	-	43.5 dBm
P1dB output power	-	33.5 dBm
$P_{sat.}$ *output power*	-	34.5 dBm
Input return loss	-	9 dB
Output return loss	-	13 dB

[a.] Is the voltage applied times the length of the phase shifter. The product is required to obtain a phase difference equal to π radians between two optical waves.

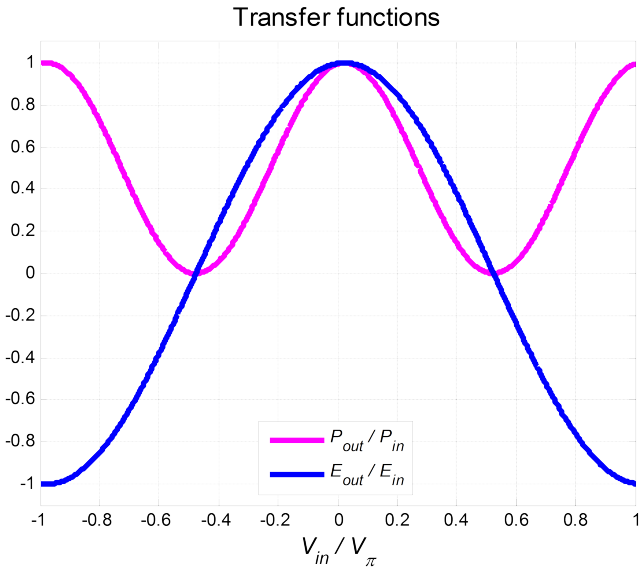

Fig. 3: Modulator transfer functions set in quadrature operating point.

Analyzing Table I, it is noted that 19 V applied to the phase shifter are required to shift the output waveform in π radians. Thus, by varying the input voltage (see Fig. 3) from -19 V to +19 V, it is possible to visualize the operating behavior of the MZM and, when necessary, to drive these curves by means of V_{DC}. The V_{DC} driving process is required to maintain the static operating curves (P_{out}/P_{in} and E_{out}/E_{in}) over the lifetime of the modulator, ensuring the modulation format performed by the RF signal.

As a result, by adjusting the device's operating point, the signal output phase was constructed to ensure destructive interference in E_{out}. Figure 4 shows the output phase of the modulator when V_{in} varies between -19 V and +19 V.

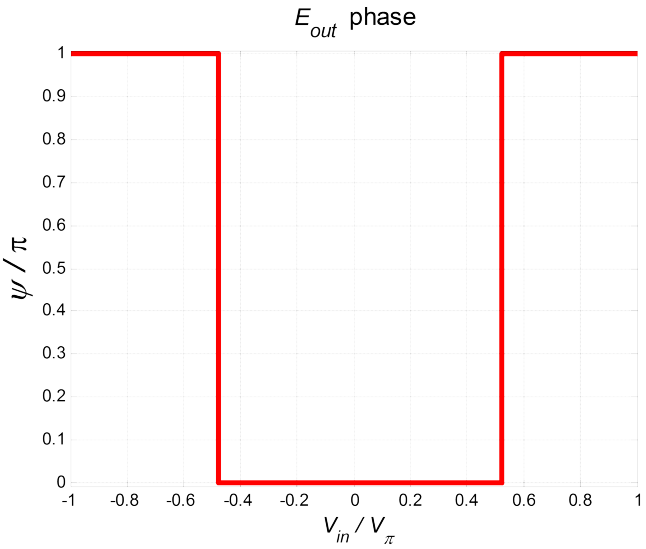

Fig. 4: Modulator phase curve set in quadrature operating point.

Note that when the V_{in}/V_π ratio is equal to ± 0.5, there is a phase shift (ψ) equal to π radians resulting from the voltages applied on the phase shifters and propagation along the waveguide (see Fig. 4). In this way, it is noted that the modulator operates in push-pull mode and causes destructive phase interference at the output signal.

B. Analysis of the electro-optical response

Taking into account the fact that the phase shifter acts on the modulator as a RC equivalent circuit, the optical response at the combiner output was calculated. Figure 5 shows how the AWG signal interferes on the optical light beam at the output of the modulator.

Note that when the signal generated by the AWG (see Fig. 5 (a)) is applied on the phase shifter, it is possible to calculate the capacitive time constant ($\tau = r_s \times C_s$) and control the signal by means of V_{in}. In this case, for τ = 0.423 ps, a square wave with pulse width equal to 25% of the period was applied, and then the expected modulation contour shape in each arm of the device was obtained (see Fig. 5(b)).

Finally, Fig. 5(c) shows destructive interference when the voltage applied to both arms of the modulator reaches maximum intensity module (9.5 V). Otherwise, when V_{in} = 0 V, the output signal does not experience an abrupt phase shift, but experiences a phase shift imposed by the total length of the waveguide. By observing a complete period of the AWG signal, it is possible to notice a robust optical intensity modulation. The expected real and ideal modulation can be compared in Figures 5(c) and 5(d), respectively.

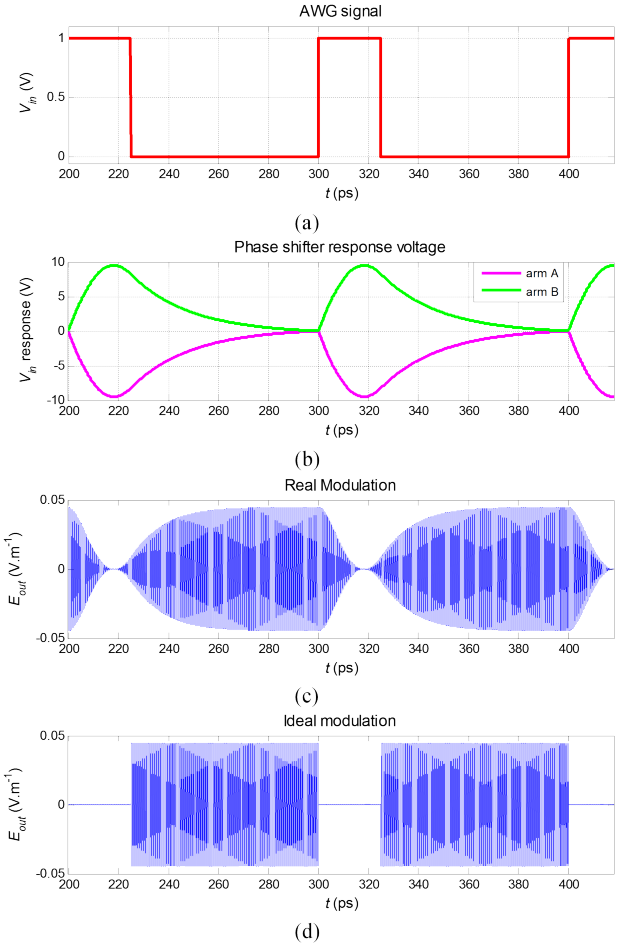

Fig. 5: Electro optical modulation signal performance. a) Voltage generated by the AWG (square wave); b) Contour shape of the modulating wave after go through the phase shifter; c) Expected optical response of the carrier wave and d) Ideal optical response of the carrier wave.

IV. Conclusion

With the increase in research directed to technologies that offer high data transmission rates, in this paper we propose design and configuration techniques of a modulator supported on ePixFab ISIPP25G silicon photonics. Based on the phase shifter device block and the RF and DC operating voltages, the study proposes means for dimensioning the length of the waveguides that make up the modulator. During this adjustment, the designer can choose between two operation means; push-pull or push-push modes. With the modulator adapted in push-pull mode and scaled to cause destructive interference to the output signal, we have shown that it is possible to induce intensity modulation with efficient figure of merit (0.95 V.cm) when the device operates at high modulation rates (20 Gb/s). For this reason, we also propose an external control circuit along with its principal electrical components (resistors, amplifier and signal generator) to act on the device's arms and ensure the desired modulation format. In this way, the external circuit can be combined with the photonic device to achieve phase or intensity modulation. Finally, the techniques used here can be implemented as paradigms in optical modulators.

References

[1] D. M. Dourado, R. J. L. Ferreira, M. de Lacerda Rocha, and U. R. Duarte, "Energy consumption and bandwidth allocation in passive optical networks," *Optical Switching and Networking*, vol. 28, pp. 1–7, 2018.

[2] A. Liu, R. Jones, L. Liao, D. Samara-Rubio, D. Rubin, O. Cohen, R. Nicolaescu, and M. Paniccia, "A high-speed silicon optical modulator based on a metal-oxide-semiconductor capacitor," *Nature*, vol. 427, pp. 615–618, February 2004.

[3] Q. Xu, B. Schmidt, S. Pradhan, and M. Lipson, "Micrometre-scale silicon electro-optic modulator," *Nature*, vol. 435, pp. 325–327, May 2005.

[4] F. Y. Gardes, G. T. Reed, G. Z. Mashanovich, and C. E. Png, *Optical Modulators in Silicon Photonic Circuits*. John Wiley & Sons Ltd, 2008.

[5] G. T. Reed and A. P. Knights, *Silicon Photonics, an Introduction*. John Wiley & Sons Ltd, 2004.

[6] Y. Kim, J. Fujikata, S. Takahashi, M. Takenaka, and S. Takagi, "First demonstration of sige-based carrier-injection mach-zehnder modulator with enhanced plasma dispersion effect," *Opt. Express*, vol. 24, no. 3, pp. 1979–1985, Feb 2016.

[7] M. J. Deen and P. K. Basu, *Silicon Photonics: Fundamentals and Devices*, 1st ed. John Wiley & Sons Ltd, 2012.

[8] M. Ziebell, "Transceiver optique en silicium pour les réseaux d'accès," Ph.D. dissertation, Universit Paris-SUD, 2013.

[9] D. Marris-Morini, V. Vakarin, P. Chaisakul, J. Frigerio, M. Rahman, J. M. Ramrez, M. Rouifed, D. Chrastina, X. L. Roux, G. Isella, and L. Vivien, "Silicon photonics based on Ge/SiGe quantum well structures," in *2016 18th International Conference on Transparent Optical Networks (ICTON)*, July 2016, pp. 1–3.

[10] G. Cocorullo and I. Rendina, "Thermo-optical modulation at 1.5 um in silicon etalon," *Electronics Letters*, vol. 28, pp. 83–85(2), January 1992.

[11] M. Seimetz, "High-order modulation for optical fiber transmission," *Springer*, vol. 143, 2009.

[12] IMEC, *imec-ePIXfab SiPhotonics: iSiPP25G*, IMEC.